Available online at www.sciencedirect.com

ScienceDirect

Geochimica et Cosmochimica Acta 71 (2007) 4814–4822

Geochimica et Cosmochimica Acta

www.elsevier.com/locate/gca

Characterisation of the magnetic iron phases in Clovis Class rocks in Gusev crater from the MER Spirit Mössbauer spectrometer

C. Van Cromphaut [a], V.G. de Resende [a], E. De Grave [a,*], A. Van Alboom [a,b], R.E. Vandenberghe [a], G. Klingelhöfer [c]

[a] *Department of Subatomic and Radiation Physics, University of Ghent, Proeftuinstraat 86, B-9000 Gent, Belgium*
[b] *Faculty of Applied Engineering Sciences, University College Ghent, Schoonmeersstraat 52, B-9000 Gent, Belgium*
[c] *Institute of Inorganic and Analytical Chemistry, Johannes Gutenberg University, Staudinger Weg 9, D-55128 Mainz, Germany*

Received 17 March 2007; accepted in revised form 30 July 2007; available online 6 September 2007

Abstract

Mössbauer backscattering spectra of eight Martian rocks, acquired by the MIMOS II spectrometer of Rover Spirit (MER-A) and containing goethite in addition to other iron minerals, have been selected for in-depth numerical analysis. Where feasible, different temperature windows for a given rock were considered. A novel calibration/folding procedure, exclusively based on the fitted positions of the eight prominent absorption lines in the transmission spectra of the reference target and not relying on the error signal of the MIMOS II spectrometer, has been developed. It is demonstrated that this procedure yields reliable and reasonably accurate values for the adjusted Mössbauer parameters of the respective spectra of the rock targets. These spectra are all composed of magnetically split components arising from hematite, magnetite and goethite phases, in addition to a ferrous and a ferric doublet that can be ascribed to the presence of Fe silicates, possibly glasses. It is argued that the Fe^{3+} doublet has no significant contribution from superparamagnetic Fe-oxide particles. The hematite components reflect the coexistence of antiferromagnetic and weakly ferromagnetic spin states. In general the magnetite content in the selected rocks is low. The goethite subspectra are very broad and asymmetric and need to be described by a model-independent distribution of hyperfine fields. The as-such obtained parameter values indicate an average particle size of the order of 10 nm. For all examined rock spectra, the adjusted parameter values for the various Fe oxides are completely in line with those known for terrestrial (natural or synthetic) species.

1. INTRODUCTION

Raw, non-calibrated backscattering Mössbauer spectra (MS) acquired in 10-K temperature windows by the two MIMOS spectrometers (Klingelhöfer et al., 2003) aboard the Mars Exploration Rovers (MER) Spirit (*MER-A*) and Opportunity (*MER-B*) are made available to the research community on several Internet sites (http://ak-guetlich.chemie.uni-mainz.de/klingelhoefer/, http://anserver1.eprsl.wustl.edu/ and http://pds.jpl.nasa.gov/). A number of research teams worldwide attempt to interpret these MS to examine the mineralogy of the Martian soils and rocks that have been the targets of the acquired MS. Various iron-bearing minerals, e.g., olivine, pyroxene, hematite and magnetite, were soon recognized during the early period of the missions (Morris et al., 2004, 2006a,b; Klingelhöfer et al., 2004). Goethite, α-FeOOH, could also be identified in some of the targets examined by *MER-A* (Klingelhöfer et al., 2005; Morris et al., 2006a). This finding supports that water has been present on the surface of Mars (Morris et al., 2006a), as goethite can be formed in an aqueous environment.

---

[*] Corresponding author.
E-mail address: eddy.degrave@Ugent.be (E. De Grave).

0016-7037/$ - see front matter © 2007 Elsevier Ltd. All rights reserved.
doi:10.1016/j.gca.2007.07.024

So far only few numerical data have been reported for the *MER-A* MS, in particular with regard to the magnetic phases Fe_3O_4 (magnetite, Mt), α-Fe_2O_3 (hematite, Ht) and α-FeOOH (Gt), and a somewhat profound characterization of these phases based on the results that have been obtained from the MS for laboratory analogs has not been established. In this contribution the interpretation is reported of a number of Spirit MS selected from the Mainz web site (http://ak-guetlich.chemie.uni-mainz.de/klingelhoefer/) on the basis of the prominent appearance of the goethite component and of the statistical quality of the spectral data of the rock and of the internal reference absorber. The latter consists of a mixture of metallic iron (α-Fe), Ht and Mt. A transmission MS of this absorber has been acquired simultaneously during each backscatter experiment.

2. METHODOLOGY

The eight selected rocks are all Clovis Class rocks (Squyres et al., 2006) and involve locations in the Columbia Hills at nearby Gusev Crater. They were already considered in previous articles (Klingelhöfer et al., 2005; Morris et al., 2006a). The target names are indicated in Table 1. Raw spectra posted for the two 14.4-keV detectors were added. For each of the eight locations, spectra in the various temperature windows were acquired repeatedly over two or more successive Martian days (*sols*, see Table 1 for specifications). As it was experienced that the reference spectra did not markedly differ between successive-sol acquisitions, the respective rock spectra for a given ΔT window and their corresponding reference spectra were summed. This is in contrast to earlier efforts in processing MER spectra (Morris et al., 2004) where reasonable counting statistics were obtained by both summing over ΔT windows and (as in this paper) by summing over the same ΔT windows for integrations done on different days. In this work, the different ΔT windows were not added together, but analysed independently when considered feasible according to the respective statistics (see Table 1).

The involved MS generally consist of two sextets due to Ht, two (minor) sextets arising from Mt, a very broad component ascribed to Gt, and a ferrous and a ferric doublet presumably due to silicates. Reliable data analyses of such complicated, multi-component MS requires proper calibration over the entire velocity range, which is not guaranteed if based on the channel position of four well-resolved absorption lines (Agresti et al., 2006) of the α-Fe phase present in the reference target and taking into account a correction based on the error signal of the drive. Because the most significant deviations from linearity of the velocity scale is experienced at the highest velocities (where the relevant Ht lines are situated), a different procedure for velocity calibration of each half and subsequent folding has therefore been worked out for this study. It merely makes use of the reference spectra, more precisely of their fitted channel positions for the six α-Fe lines and for the two outer Ht lines. Since reference hyperfine data for the individual phases constituting the actual calibration target have, as far as known, not been released, an absorber was prepared consisting of a thin iron foil on which a layer of well-crystallized Ht powder was deposited. Using this absorber, the MER transmission runs for the reference target were mimicked in the laboratory, including the gradual change of temperature in each relevant ΔT window. It is evident that for the α-Fe foils used in the MER and in the laboratory reference targets the hyperfine parameters will not significantly differ. The same invariability is most likely true for the Ht phase present in the two targets. The observation that the Morin-transition temperature for the Ht phase of the MER reference target is relatively high indeed implies that the involved Ht particles exhibit a reasonably high degree of crystallization, similar to that of the Ht particles in the laboratory reference absorber, so that within the error limits of the MER experiments, the Ht hyperfine parameters at any given temperature may be considered identical. Therefore, the authors are confident that the hyperfine parameters, and hence the resonant velocities v_0 of the respective absorption lines, as obtained from the MS of the laboratory reference absorber in the respective ΔT windows, can be safely used for calibration purposes of the MER spectra.

Details about the developed velocity-calibration and folding procedure for the MS of the rock targets are given in (see electronic annex). An ultimate test for the validity of the calibration/folding procedure consisted of processing, according to that procedure, a spectrum of the reference target as if it were a transmission spectrum of a Martian rock target. Fig. 1 shows the calibration spectrum associated with the Spirit MS of Clovis rock (sols 212–223), ΔT window m5, obtained by adding together ten m5 reference-target spectra. Using conventional software, five symmetrical Lorentzian sextets were successfully fitted to the data: (i) an α-Fe sextet with two width parameters [intrinsic width Γ and broadening parameter $\Delta\Gamma$ (Vandenberghe et al., 1994)] and quadrupole shift $2\varepsilon_Q$ forced to be zero; (ii) two α-Fe_2O_3 sextets [antiferromagnetic (AF) and weak ferromagnetic (WF) contributions, the coexistence of which in the temperature range of the Morin transition is well documented] with equal width and broadening parameters, equal isomer-shift values, and both with fixed 3:2:1 ratios for the outer to middle to inner line areas for each sextet; and (iii) two Fe_3O_4 sextets (tetrahedral Fe^{3+} and octahedral

Table 1
Rocks, whose Mössbauer spectra have been evaluated, sol numbers corresponding to these spectra, and temperature windows considered in this report

Target name	Sol numbers	Temperature windows[a]
Clovis	212–223	m5, m6, m7, m89
Ebenezer–Ratchit 2	232–234	m5, m6
Ebenezer–Cratchit	229, 230	m5, m6
Wooly Patch	193–200	m5
Uchben	284–292	m5, m6, m7
Temples	268–270	m5
Watchtower	417–419	m5
Lutefisk	298–302	m5

[a] m5: 210–220 K, m6: 220–230 K, m7: 230–240 K, m89: 240–260 K.

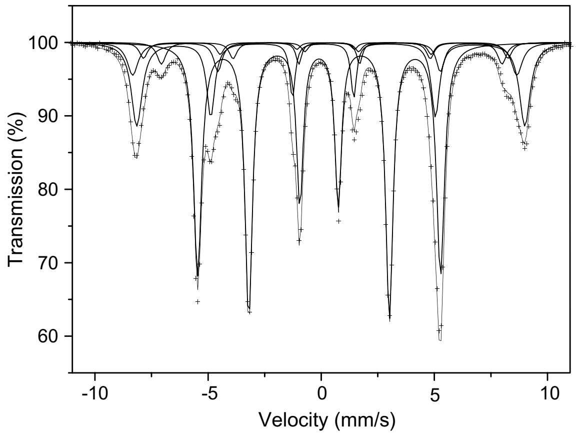

Fig. 1. Mössbauer spectrum of the Spirit reference target acquired while examining Clovis rock in the ΔT window m5. The experimental data (+) are the summation of ten runs (sols 212–223). The solid lines are the five different sextet components resolved from the spectrum and their sum.

$Fe^{2.5+}$ contributions, respectively, A and B sites) also with fixed 3:2:1 area ratios, zero quadrupole shifts and 1:1.8 area ratio for the Fe^{3+} contribution with respect to the $Fe^{2.5+}$ contribution (De Grave et al., 1993). The as such calculated sum spectrum is shown by a solid line in Fig. 1. The adjusted hyperfine parameters are listed in Table 2 and compared with the results measured for laboratory samples, i.e., the aforementioned α-Fe/α-Fe_2O_3 reference absorber (results for α-Fe and for the AF contribution by α-Fe_2O_3, window m5), for a natural terrestrial Ht (results for α-Fe_2O_3—WF at $T = 215$ K) (De Grave and Vandenberghe, 1990), and for stoichiometric Fe_3O_4 at 215 K (De Grave et al., 1993). The area ratios for the outer to middle to inner absorption lines for the α-Fe sextet were found to be 3:3.3:1, reflecting the preferential orientation of the spins for the plane of the foil, which is not unusual. In general, the hyperfine parameters found for the various Fe-bearing phases in Spirit's reference target are in reasonable agreement with the data obtained for the laboratory analogs, thus supporting the applied calibration and folding procedure. The slightly lower δ value for the Mt component corresponding to the octahedral $Fe^{2.5+}$ species, δ_B, for the MER reference target as compared to the value for the laboratory target (0.59 mm/s versus 0.65 mm/s, respectively; see Table 2) is likely to be due to the strong overlap of the various sextets and the weak intensities of the Mt components, causing the latter to be ill-resolved. As a consequence, it may be expected that not all of the adjusted parameter values for the two Mt subspectra are sharply defined. A trial fit of the spectrum shown in Fig. 1, with $\delta_B = 0.65$ mm/s fixed in the iteration, yielded an equally adequate reproduction of the experimental data with no significant effect on the adjusted values for the other Mössbauer parameters.

It is worth mentioning that similar processing of the reference spectra was also performed for the three other temperature windows for Clovis rock. These results equally well support the proposed calibration approach. The following results also show that less hyperfine parameters were being kept fixed during iteration as compared to the results based on other calibration methods (Klingelhöfer et al., 2005; Morris et al., 2006a).

3. RESULTS

During the second part of this work the MS of the rocks listed in Table 1 were analysed. As mentioned above, these spectra are composed of two doublets and three magnetic components due to the presence of iron oxides. First, the results for the temperature window m5 of all eight targets are presented. Exemplary experimental and calculated spectra are shown in Fig. 2, referring to spectra of Ebenezer–Ratchit rock. Apart from the relative fractional areas of the various components, the MS of the other rocks are all similar (see EA). It should be repeated at this point that each spectrum considered was calibrated/folded using the reference target spectrum that was acquired simultaneously with the MS for the rock target itself.

3.1. Hematite

In the course of the attempting to fit the m5 spectra, it soon became clear that, apart from the Wooly Patch and Temples rocks, the Ht sextets for all other rocks considered in this report consist of AF and WF contributions. An obvious indication of the co-existence of the two spin states is the significant asymmetry in peak depths and line width

Table 2

Fitted Mössbauer parameters of the various Fe phases present in the MER-A reference target for the added-together spectra acquired of this target in the temperature window m5 while measuring the backscatter spectra of the Clovis rock

Fe phase	*MER-A* reference target			Laboratory target		
	B_{hf} (T)	δ (mm/s)	$2\varepsilon_Q$ (mm/s)	B_{hf} (T)	δ (mm/s)	$2\varepsilon_Q$ (mm/s)
α-Fe	33.3	0.02	0.0[a]	33.3	0.00	0.0[a]
α-Fe_2O_3-AF	53.2	0.36	0.34	53.4	0.37	0.39
α-Fe_2O_3-WF	52.6	0.36	−0.19	52.5	0.38	−0.14
Fe_3O_4-oct.	46.5	0.59	0.0[a]	46.9	0.65	0.0
Fe_3O_4-tetr.	50.0	0.28[a]	0.0[a]	49.8	0.27	0.0

The experimental sum spectrum was obtained after calibration/folding according to the method described in (see EA). The three columns at the right contain the results derived from the MS of terrestrial laboratory samples for similar temperature conditions. B_{hf} refers to the magnetic hyperfine field, δ to the isomer shift and $2\varepsilon_Q$ to the quadrupole shift.

[a] Parameter values fixed in the iteration.

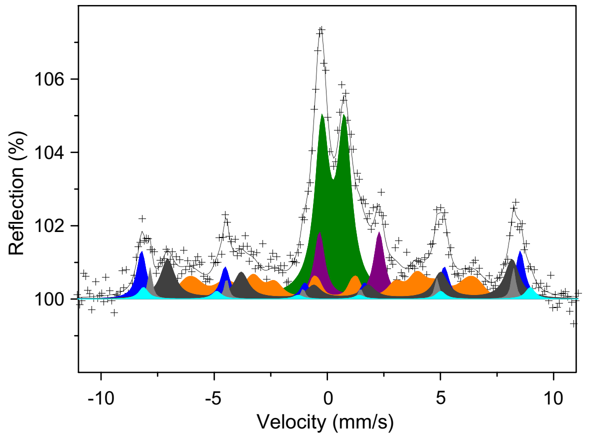

Fig. 2. Experimental (+) and fitted (solid line) Mössbauer spectrum of Ebenezer–Ratchit 2 rock acquired in the temperature window m5 (210–220 K). Colour codes: hematite WF state (blue), hematite AF state (cyan), magnetite tetrahedral Fe^{3+} (light grey), magnetite octahedral $Fe^{2.5+}$ (dark grey), goethite (orange), Fe^{3+} doublet (green) and Fe^{2+} doublet (purple).

of the outer lines of the hematite contribution (see Fig. 2 for an example). This asymmetry is also observed in the MS shown by Morris et al. (2006a); however, these authors did not attempt to resolve the two components for the these rocks, presumably because of too low intensity of the overall Ht signal. In this work, discrete Lorentzian-shaped sextets were used for each of the two Ht contributions and the same restrictions were imposed as those mentioned earlier for the numerical processing of the spectra of the reference targets, i.e., equal isomer shifts and line width parameters Γ and $\Delta\Gamma$ for AF and WF sextets and a 3:2:1 area ratio for the outer to middle to inner lines. In addition, it was found necessary to fix the quadrupole shifts of the AF component in order for the iteration program to reach proper convergence. The reasonable value of 0.36 mm/s for $2\varepsilon_{Q,AF}$ was found to be adequate. The exact value, however, has little impact on the final values of the various other Mössbauer parameters because of the generally weak signal arising from the AF contribution, i.e., barely 5% of the total spectral area. The thus obtained numerical results from fitting of the Ht components are summarized in Table 3. It is noticed that the Ht parameters for the eight rocks are fairly consistent and totally in line with parameter values for laboratory species. The reader may argue that the scatter, particularly for the B_{hf} data, seems to be significant. We believe it is not, considering the rather poor resolution and low counting statistics of both target and corresponding calibration spectra. Each channel represents a velocity interval of the order of 0.1 mm/s, which, on a hyperfine-field scale, represents 0.3 T. A systematic error on the adjusted hyperfine field results of 0.5 T seems not to be overestimated considering the poor statistics of the spectra. Hence, one may conclude that $B_{hf,WF}$ (WF state) equals 52.4 ± 0.5 T and $B_{hf,AF}$ (AF state) 53.3 ± 0.5 T, which compare well with the field values of the laboratory samples reported in Table 2.

Similar results were obtained for the isomer shifts of hematite by Morris et al. (2006a) in cases where the Ht component is more prominent and was decomposed into the two phases, but these authors mention larger differences (up to 2 T) between the hyperfine fields of the WF and AF phase than those commonly observed in the laboratory for natural terrestrial hematite (0.8 T, e.g., De Grave and Vandenberghe, 1990). Further, the quadrupole shifts mentioned by Morris et al. (2006a) and by Dyar et al. (2006) are average values for the involved temperature range (210–260 K), in which these values can vary significantly between −0.20 and −0.01 for the WF phase, and between 0.00 and 0.44 for the AF phase (De Grave and Vandenberghe, 1990). In contrast, the quadrupole shift values mentioned in the present paper refer to a narrower temperature range and show much resemblance to those of natural hematites on Earth (−0.20 and 0.36 mm/s) (De Grave and Vandenberghe, 1990). Finally, Klingelhöfer et al. (2005) reported fixed values for the isomer shift of hematite at 0.416 mm/s, which are unacceptably high for a natural hematite at the mentioned temperatures (220–260 K) and when source and target are kept at the same temperature.

3.2. Magnetite

To resolve the two sextets of the Mt components, narrow, model-independent hyperfine-field distributions (HFD) were used for both sites. In this way, the field values were forced to be close to the values that were found for synthetic magnetites. It is known that these values are not significantly affected by a moderate oxidation of Fe on the B sites (da Costa et al., 1995a). In several cases where discrete sextets were imposed, the adjusted field parameters were found to be physically unrealistic. Field ranges of 49.5–50.5 and of 46.5–47.5 T, both in increments of 0.1 T, were chosen for the A and B sites, respectively. Quadrupole shifts were forced to be zero and for some spectra with a weak contribution from the Mt phase, the isomer shifts had to be constrained as well. The obtained Mt parameters are listed in Table 3. For the Watchtower rock no Mt contribution could be detected.

With the exception of the A-site hyperfine field for the Lutefisk rock, all other Mt hyperfine parameters derived from the MER spectra are in excellent agreement with the results known for pure laboratory Mt at the mid-point temperature of 215 K (see Table 2). Due to the generally weak contribution of the Mt signal, the relative spectral areas are ill-defined, and conclusions concerning a possible partial oxidation of the mixed-valence iron oxide cannot be drawn. Similar results for Mt at these sites were found by Morris et al. (2006a) and Ming et al. (2006) (2% for Clovis) but the relevant hyperfine parameters were kept fixed during iteration or not mentioned, respectively.

3.3. Goethite

The broad Gt components were fitted with a hyperfine field distribution (HFD) spanning the range 20 to 45 T in increments of 1 T. Initial attempts to adjust the Gt component using a HFD interval of 10–45 T showed that a lower limit of 20 T is a reasonable choice. Average isomer and quadrupole shifts and the elemental line widths were

Table 3
Relevant Mössbauer parameters for the goethite, hematite, magnetite, ferrous and ferric doublet components present in the spectra acquired in the m5 temperature windows (210–220 K) of several Gusev Crater rocks

Target name	Goethite					Hematite						
						WF phase				AF Phase		
	$B_{\mathrm{hf,m1}}$ (T)	$B_{\mathrm{hf,m2}}$ (T)	δ^{b} (mm/s)	$2\varepsilon_Q$ (mm/s)	S	δ^{b} (mm/s)	B_{hf} (T)	$2\varepsilon_Q$ (mm/s)	S	B_{hf} (T)	$2\varepsilon_Q$ (mm/s)	S
Clovis	37.3	31.0	0.40	−0.18	0.40	0.37	52.6	−0.16	0.09	53.3	0.36[a]	0.06
Eb[c].–Cratchit	38.0	30.1	0.36[a]	−0.26	0.18	0.34	51.9	−0.15[a]	0.12	53.1	0.36[a]	0.06
Eb[c].–Ratchit 2	38.5	28.8	0.36[a]	−0.19	0.20	0.35	51.9	−0.17	0.13	53.0[a]	0.36[a]	0.03
Wooly Patch	36.9	29.2	0.40	−0.26[a]	0.12	0.40	51.9	−0.11	0.13	—	—	—
Uchben	38.8	30.2	0.36[a]	−0.25	0.27	0.40	52.8	−0.15[a]	0.07	53.7	0.36[a]	0.03
Temples	38.0	30.3	0.38	−0.27	0.25	0.38	52.3	−0.18	0.18	—	—	—
Watchtower	38.1	29.6	0.36[a]	−0.17	0.13	0.38	53.0	−0.15[a]	0.06	54.0	0.36[a]	0.27
Lutefisk	37.6	28.0	0.37	−0.18	0.17	0.39	52.5	−0.14[a]	0.12	53.7	0.36[a]	0.03

	Magnetite						Ferrous doublet			Ferric doublet		
	A site			B site								
	B_{hf}^{Δ} (T)	δ^{b} (mm/s)	S	B_{hf}^{Δ} (T)	δ^{b} (mm/s)	S	ΔE_Q (mm/s)	δ^{b} (mm/s)	S	ΔE_Q (mm/s)	δ^{b} (mm/s)	S
Clovis	49.8	0.26	0.01	47.2	0.66§	0.02	2.29	1.14	0.14	1.07	0.33	0.27
Eb[c].–Cratchit	49.9	0.31	0.05	47.1	0.62	0.15	2.33	1.13	0.14	1.07	0.33	0.30
Eb[c].–Ratchit 2	49.8	0.31	0.04	47.2	0.68	0.17	2.64	1.08	0.10	1.01	0.37	0.34
Wooly Patch	50.2	0.35	0.08	46.9	0.62	0.06	2.16	1.15	0.31	0.89	0.34	0.31
Uchben	50.1	0.28[a]	0.06	46.6	0.66	0.06	2.69	1.20	0.15	0.91	0.40	0.37
Temples	49.8	0.28	0.02	47.2	0.65	0.04	2.25	1.14	0.20	1.01	0.35	0.32
Watchtower	—	—	—	—	—	—	2.79	1.03	0.15	0.92	0.34	0.40
Lutefisk	50.6	0.27	0.11	47.0	0.69	0.10	2.27	1.02	0.24	1.04	0.34	0.22

The hyperfine field $B_{\mathrm{hf,m}}$ refers to the maximum-probability hyperfine field, δ to the isomer shift, $2\varepsilon_Q$ to the quadrupole shift and S to the fraction spectral area of the total spectrum, being approximately the fraction of Fe species in the respective sites.

[a] Parameter value fixed in the iteration.

[b] Referred to α-Fe at the same temperature.

[c] Ebenezer rock.

generally adjustable parameters. Again the outer to middle to inner line area ratios of the composing sextets were fixed at 3:2:1. The as such obtained relevant Mössbauer parameters are presented in Table 3. For comparison, a sample (GPC0A) out of several goethites synthesized under various conditions and according to methods reported in the literature (Schwertmann and Cornell, 1991), was found with similar hyperfine parameters ($B_{\mathrm{hf,m}}$: 39.2 T, $B_{\mathrm{hf,av}}$: 32.8 T, δ: 0.36 mm/s and $2\varepsilon_Q$: −0.25 mm/s).

The hyperfine field, and to a lesser extent also the quadrupole shift, of terrestrial goethites (natural and synthetic) at the relevant temperature range is very sensitive to the morphology of the particles and varies from ~45 T for well crystalline species (De Grave and Vandenberghe, 1986) to 0 T for small-particle (superparamagnetic) and/or Al-substituted Gt. The observed field values for the Martian goethites of on average $H_{\mathrm{hf,m}} \approx 37$ T would thus indicate a particle size of around 10 nm (which is the estimated size for the GPC0A particles) assuming no significant Al-for-Fe substitution. The hyperfine field of goethite in the Clovis rock is in the same range as the one found by Morris et al. (2006a). As stressed in the Discussion section hereafter, this hyperfine field is very sensitive to temperature changes (increase of 1.4 T in the temperature range 210–260 K). The results of Klingelhöfer et al. (2004) show an even larger temperature dependence of the hyperfine field (2.7 T in the same range). Therefore, we prefer to analyse the spectral data collected for only one temperature window. Furthermore, this approach has led to quadrupole shift values of around −0.25 mm/s which are indeed much closer to the quadrupole shifts of natural goethites (Murad and Johnston, 1987) than those found by Morris et al. (2006a), i.e., −0.17 mm/s.

In the present report, the presence of goethite in other rocks from the Clovis Class is also proven without fixing the hyperfine parameters, in contrast to Morris et al. (2006a) who fixed these hyperfine parameters at 36.5 T, −0.17 and 0.38 mm/s for the hyperfine field, quadrupole shift and isomer shift, respectively.

A remarkable finding concerning the HFDs ascribed to Gt is that the evaluated probability distribution profiles $p(H_{\mathrm{hf}})$ are bimodal. The most illustrative and striking example of this feature is shown in Fig. 3. For most other rocks in the various temperature windows the existence of two maxima in $p(H_{hf})$ is less resolved and in some cases only appears as a weak low-field shoulder on a main component. However, for all spectra considered in this report, the obtained HFD profiles could be described by a superposition of two Gaussian curves. From this conclusion one could infer that the distributions of particle sizes of the Martian Gt phases are bimodal, part having a smaller average size, another part having a distinctively larger size, or that both fractions are characterized by significantly different amounts of Al substitution. Since the particle size of Gt is primarily determined by the chemical environment during crystal growth, this might imply that in the history of Mars some change in the climatological and/or environmental conditions could have occurred.

On the other hand, the bimodal appearance of the $p(H_{\mathrm{hf}})$ curves could instead be the result of the presence, in addition to Gt, of another iron phase with distributed hyperfine field. Merely on the basis of the Mössbauer characteristics of the broad sextet component, a possible candidate in that respect would be poorly crystalline maghemite, γ-Fe_2O_3. The principal pathway for the formation of terrestrial maghemite is by oxidation of Mt (Cornell and Schwertmann, 2003), which requires a sufficient abundance of oxygen. This is currently not the case and hence, if maghemite is indeed present, this also would indicate a change in the environmental conditions at some time in the history of the planet. Clear-cut evidence that γ-Fe_2O_3 is or is not in the involved rocks cannot be obtained from their MS. Attempts to include in the fitting approach a HFD representing poorly crystalline γ-Fe_2O_3, with fixed parameters typical of that phase, i.e., $\delta = 0.23$ mm/s and $2\varepsilon_Q = 0.00$ mm/s (da Costa et al., 1995b), were unsuccessful.

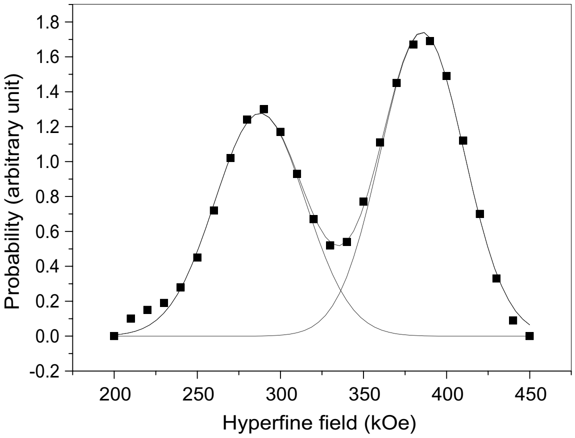

Fig. 3. The hyperfine-field-distribution profile (solid squares) of the part of the Mössbauer spectrum for Ebenezer–Ratchit rock ascribed to goethite. The solid lines are the Gaussian curves and their superposition as adjusted to the evaluated profile.

3.4. Ferrous and ferric doublet

The doublet components present in the Gusev MS were have here been described by symmetrical quadrupole doublets with no restrictions imposed on the Mössbauer parameters that had to be adjusted. The values of these parameters obtained from the fits are listed in Table 3. There is consensus in the literature (Morris et al., 2006a; Dyar et al., 2006) that the assignment of the doublet signals to particular Fe phases is not straightforward, and we agree with earlier statements in that respect. Concerning the ferrous doublet, possible candidates have been suggested to be pyroxene, olivine, or some hydrous sulphates (Morris et al., 2004; Dyar et al., 2006). The present numerical results do not provide a decisive answer in that respect. As for the ferric doublet, Morris et al. (2004, 2006a) have claimed that this doublet is due to nanophase ferric oxide particles (npOx) which is a generic name for oct-Fe^{3+} doublets from phases that are Fe^{3+}-bearing products of oxidative weathering. Terrestrial poorly crystalline Fe^{3+} oxides or oxyhydroxides (whether environmental or synthetic) have never shown a quadrupole splitting of as much as 1.1 mm/s as observed for the ferric doublet present in the investigated Spirit MS investigated in this work. A possibility that has received little attention so far is that the doublets are due to the presence of Fe^{2+}- and Fe^{3+}-containing silicate glasses. The MS-parameter values resulting from the fits (Table 3) indeed bear close resemblance to those obtained for silicate glasses used for the conditioning of low-level radioactive waste products (De Grave and Van Iseghem, 1986). Considering the geological history of the location (i.e., an old volcano crater, Herkenhoff et al., 2004) at which the involved Spirit MS were recorded, the occurrence of Fe-bearing glassy substances is plausible.

Morris et al. (2006a) mentioned for the same rocks the presence of three doublets: the first two (a ferric and ferrous doublet with average quadrupole splitting of 1.0 and 2.2 mm/s) show much resemblance to the two doublets discussed here, and, moreover, have similar spectral areas. The third doublet, which was attributed to olivine, was fitted with all parameters fixed and its spectral area was consistently found to be less than 4%. In our work, no indication of this doublet was found.

4. DISCUSSION AND CONCLUSION

As Table 1 indicates, the MER MS for Clovis rock acquired at four consecutive temperature windows have been analysed in this work, providing the opportunity to examine the consistency of the temperature-related variations of the Mössbauer parameters of the various Fe phases present in this rock, and to evaluate a new calibration/folding procedure. The involved raw data were processed and subsequently fitted in exactly the same way for all four spectra. The experimental and calculated spectra and the distinct components are reproduced in Fig. 2 in the EA.

In general, the variations of the hyperfine parameters of Ht and Mt in the involved temperature range, i.e., ~210–260 K, are relatively small. For instance, for a natural sample of terrestrial Ht the hyperfine fields were found to decrease systematically with increasing temperature from 52.3 to 52.0 T and from 53.0 to 52.5 T for WF and AF spin states, respectively (De Grave and Vandenberghe, 1990). For the quadrupole shifts, the corresponding ranges are between −0.14 and −0.19 mm/s and between 0.36 and 0.30 mm/s. Although the Ht parameters for the Clovis rock are in good agreement with the above, their variations are less systematic and more or less scattered instead. This scatter is likely due to a combination of several factors: complexity of the spectra, poor counting statistics, and a resolution that is lower than common for laboratory MS. As a result of these adverse factors, the adjustment values for the various Mössbauer parameters are relatively uncertain.

The hyperfine fields of terrestrial goethites at Martian temperatures cover a broad range of values depending on the morphology, particle diameter and Al substitution. The Clovis Gt phase is most probably composed of small particles, somewhat less than 10 nm in size. The effect of lowering the Gt hyperfine field upon increasing the temperature from ~215 to ~250 K is significantly more enhanced than for Ht and Mt. This is clearly reflected in the adjusted values of the maximum-probability field, $B_{hf,max}$, as listed in Table 4. Within experimental uncertainties, the other Mössbauer parameters (δ, $2\varepsilon_Q$ and S) remain unchanged for the four temperature windows.

Consistent variations, or lack of variations, for the doublet' parameters over the four temperature windows for the Clovis rock (Table 4) nicely corroborate the calibration/folding procedure as developed by us for the MER Spirit MS. The finding that the fractional spectral area of the ferric doublet remains unchanged on lowering the temperature is an indication that there are no superparamagnetic Gt particles present in the Clovis target at the involved temperatures.

Dyar et al. (2006) mentioned the hyperfine parameters of several iron oxides measured by MER-B (Opportunity), though a specific identification of the different iron oxides in each rock has not yet been performed, nor are fitted Mössbauer spectra available. Morris et al. (2006a) gave an extended overview of all rocks measured by MER-A, but there are some significant differences with the results of this work. These differences are the result of a different approach for calibration and folding on the one hand, and from a different fitting procedure. The method as described in this manuscript uses the outer hematite lines of the reference sample, ensuring a proper calibration at high velocities which is not assured by the method of Agresti et al. (2006). The calibration method is also the only approach which does not rely on the error signal, and it is the first one reported that analyzes spectra acquired in merely one temperature window (10 K), instead of considering a summation of all spectra obtained for a given target in all available temperature windows. The new procedure leads to more specific (i.e., averaged over a more narrow temperature window) values for the hyperfine parameters such as the hyperfine field and quadrupole shift of the components assigned to goethite and hematite. Moreover, some additional improvements to the fitting procedure have been made such as the fit of the hematite spectral component by two instead of one spin state, which is necessary because of the obvious and significant asymmetry of the hematite lines in most of the spectra reproduced in both the present study and in some of the earlier reports. Further, as compared to fitting approaches used in any of the previous articles, less hyperfine-parameter values had to be fixed in our iterations.

This paper makes a contribution to the research of the MER Mössbauer spectroscopy, concerning the iron oxides present on Mars. A novel calibration procedure was developed, allowing single-temperature window analysis and yielding reliable results from the as-such processed spectra. The obtained parameter values for the iron oxides present in the selected rocks are all consistent with results obtained for terrestrial species. The developed calibration procedure has also allowed to resolve (with acceptable parameter values) the subspectra due to the two magnetic states present in the Ht phase. In addition, Gt was observed in all investigated rocks, and its spectral component could be adequately described imposing a minimum of constraints on the hyperfine parameters. This work has allowed to detect a bimodal distribution for the hyperfine field parameter suggesting different particle size and/or Al substitution.

Table 4

Relevant Mössbauer parameters for the components present in the spectra acquired for Clovis rock in the m5, m6, m7 and m89 temperature windows

Window	Goethite					Hematite						
						WF phase				AF Phase		
	$B_{hf,m1}$ (T)	$B_{hf,m2}$ (T)	δ^{b} (mm/s)	$2\varepsilon_Q$ (mm/s)	S	δ^{b} (mm/s)	B_{hf} (T)	$2\varepsilon_Q$ (mm/s)	S	B_{hf} (T)	$2\varepsilon_Q$ (mm/s)	S
m5	37.3	31.0	0.40	−0.18	0.40	0.37	52.6	−0.16	0.09	53.3	0.36[a]	0.06
m6	36.9	31.0	0.39	−0.19	0.40	0.39	52.8	−0.15	0.10	53.4	0.34[a]	0.05
m7	36.7	30.9	0.36	−0.17	0.38	0.34	52.6	−0.19	0.11	53.5	0.31[a]	0.07
m89	35.9	29.8	0.37	−0.22	0.38	0.35	52.7	−0.14	0.15	—	—	—

Window	Magnetite						Ferrous doublet			Ferric doublet		
	A site			B site								
	B_{hf} (T)	δ^{b} (mm/s)	S	B_{hf} (T)	δ^{b} (mm/s)	S	ΔE_Q (mm/s)	δ^{b} (mm/s)	S	ΔE_Q (mm/s)	δ^{b} (mm/s)	S
m5	49.8	0.26	0.01	47.2	0.66[a]	0.02	2.29	1.14	0.14	1.17	0.33	0.27
m6	50.2	0.32	0.02	46.8	0.67	0.02	2.27	1.16	0.14	1.16	0.33	0.27
m7	50.3	0.28[a]	0.01	46.8	0.66[a]	0.01	2.23	1.14	0.15	1.14	0.36	0.26
m89	50.2	0.28[a]	0.01	46.8	0.66[a]	0.01	2.25	1.18	0.14	1.15	0.36	0.27

The hyperfine field $B_{hf,m}$ refers to the maximum-probability hyperfine field, δ to the isomer shift, $2\varepsilon_Q$ to the quadrupole shift and S to the fraction spectral area of the total spectrum, being approximately the fraction of Fe species in the respective sites.

[a] Parameter value fixed in the iteration.

[b] Referred to α-Fe at the same temperature.

Olivine was not observed in the MS from any of the analyzed rocks.

ACKNOWLEDGMENT

The authors would like to thank FWO-Vlaanderen for financial support.

APPENDIX A. SUPPLEMENTARY DATA

Supplementary data associated with this article can be found, in the online version, at doi:10.1016/j.gca.2007.07.024.

REFERENCES

Agresti D. G., Dyar M. D. and Schaefer M. W. (2006) Velocity scales for Mars Mössbauer data. *Hyperfine Interact.* **170**, 67–74.

Cornell R. M. and Schwertmann U. (2003) *The Iron Oxides*, second ed. Wiley-VCH Verlag, Weinheim.

da Costa G. M., De Grave E., de Bakker P. M. A. and Vandenberghe R. E. (1995a) Influence on nonstoichiometry and the presence of maghemite on the Moessbauer spectrum of magnetite. *Clay Clay Miner.* **43**, 656–668.

da Costa G. M., De Grave E., Bowen L. H., de Bakker P. M. A. and Vandenberghe R. E. (1995b) Variable-temperature Mössbauer spectroscopy of nano-sized maghemite and Al-substituted maghemites. *Clay Clay Miner.* **43**, 562–568.

De Grave E. and Van Iseghem P. (1986). In *Industrial Applications of the Mössbauer Effect* (eds. G. J. Long and J. G. Stevens). Plenum Press, New York, pp. 423–446.

De Grave E. and Vandenberghe R. E. (1986) ^{57}Fe Mössbauer effect study of well-crystallized goethite (α-FeOOH). *Hyperfine Interact.* **28**, 643–646.

De Grave E. and Vandenberghe R. E. (1990) Mössbauer effect study of the spin structure in natural hematites from the region of Elba. *Phys. Chem. Miner.* **17**, 344–352.

De Grave E., Persoons R. M., Vandenberghe R. E. and de Bakker P. M. A. (1993) Mössbauer study of the high-temperature phase of Co-substituted magnetites, $Co_xFe_{3-x}O_4$. I. $x \leqslant 0.04$. *Phys. Rev. B* **47**, 5881–5893.

Dyar, M.D., Rothstein, Y., Schaefer, M.W. and Agresti, D.G. (2006) Mössbauer spectroscopy of outcrop at the Meridiani Planum site. LPSC XXXVII, Abstract #2382.

Herkenhoff K. E., Squyres S. W., Arvidson R., Bass D. S., Bell J. F., Bertelsen P., Cabrol N. A., Gaddis L., Hayes A. G., Hviid S. F., Johnson J. R., Kinch K. M., Madsen M. B., Maki J. N., McLennan S. M., McSween H. Y., Rice J. W., Sims M., Smith P. H., Soderblom L. A., Spanovich N., Sullivan R. and Wang A. (2004) Textures of the soils and rocks at Gusev crater from spirit's microscopic imager. *Science* **305**, 824–826.

Klingelhöfer G., Morris R. V., Bernhardt B., Rodionov D., De Souza P. A., Squyres S. W., Foh J., Kankeleit E., Bonnes U., Gellert R., Schröder C., Linkin S., Evlanov E., Zubkov B. and Prilutski O. (2003) Athena MIMOS II Mossbauer spectrometer investigation. *J. Geophys. Res.* **108**(E12), 8067–8084.

Klingelhöfer G., Morris R. V., Bernhardt B., Schroder C., Rodionov D. S., de Souza P. A., Yen A., Gellert R., Evlanov E. N., Zubkov B., Foh J., Bonnes U., Kankeleit E., Gutlich P., Ming D. W., Renz F., Wdowiak T., Squyres S. W. and Arvidson R. E. (2004) Jarosite and hematite at Meridiani Planum opportunity's Mössbauer spectrometer. *Science* **306**, 1740–1745.

Klingelhöfer G., De Grave E., Morris R. V., Van Alboom A., de Resende V. G., De Souza, Jr., P. A., Rodionov D., Schröder C., Ming D. W. and Yen A. (2005) Mössbauer spectroscopy on Mars: goethite in the Columbia hills at Gusev crater. *Hyperfine Interact.* **166**, 549–554.

Ming D. W., Mittlefehldt D. W., Morris R. V., Golden D. C., Gellert R., Yen A., Clarck B. C., Squyres S. W., Farrand W. H., Ruff S. W., Arvidson R. E., Klingelhöfer G., McSween H. Y., Schröder C., Rodionov D. S., de Souza P. A. and Wang A. (2006) Geochemical and mineralogical indicators for aqueous processes in the Columbia Hills of Gusev crater. *Mars J. Geophys. Res.* **111**, E02S12.

Morris R. V., Klingelhöfer G., Bernhardt B., Schroder C., Rodionov D. S., de Souza P. A., Yen A., Gellert R., Evlanov E. N., Foh J., Kankeleit E., Gutlich P., Ming D. W., Renz F., Wdowiak T., Squyres S. W. and Arvidson R. E. (2004) Mineralogy at Gusev crater from the Mossbauer spectrometer on the spirit rover. *Science* **305**, 833–836.

Morris R. V., Klingelhöfer G., Schroder C., Rodionov D. S., Yen A., Ming D. W., de Souza P. A., Fleischer I., Wdowiak T., Gellert R., Bernhardt B., Evlanov E. N., Zubkov B., Foh J., Bonnes U., Kankeleit E., Gutlich P., Renz F., Squyres S. W and Arvidson R. E. (2006a) Mössbauer mineralogy of rock, soil, and dust at Gusev crater, Mars: spirit's journey through weakly altered olivine basalt on the plains and pervasively altered basalt in the Colombia Hills. *J. Geophys. Res.* **111**, E02S13.

Morris R. V., Klingelhöfer G., Schroder C., Rodionov D. S., Yen A., Ming D. W., de Souza P. A., Wdowiak T., Fleischer I., Gellert R., Bernhardt B., Bonnes U., Cohen B. A., Evlanov E. N., Foh J., Gutlich P., Kankeleit E., McCoy T., Mittlefehldt D. W., Renz F., Schmidt M. E., Zubkov B., Squyres S. W. and Arvidson R. E. (2006b) Mössbauer mineralogy of rock, soil, and dust at Meridiani Planum, Mars: opportunity's journey across sulfate-rich outcrop, basaltic sand and dust, and hematite lag deposits. *J. Geophys. Res.* **111**, E12S15.

Murad E. and Johnston J. H. (1987) Iron oxides and oxyhydroxides. In *Mössbauer Spectroscopy Applied to Inorganic Chemistry*, vol. 2 (ed. G. J. Long). Plenum Press, New York, pp. 507–582.

Schwertmann U. and Cornell R. M. (1991) *Iron Oxides in the Laboratory*. VCH Verlagsgesellschaft, Weinheim.

Squyres S. W., Arvidson R. E., Blaney D. L., Clark B. C., Crumpler L., Farrand W. H., Gorevan S., Herkenhoff K. E., Hurowitz J., Kusack A., McSween H. Y., Ming D. W., Morris R. V., Ruff S. W., Wang A. and Yen A. (2006) Rocks of the Columbia Hills. *J. Geophys. Res.* **111**, E02S11.

Vandenberghe R. E., De Grave E. and de Bakker P. M. A. (1994) On the methodology of the analysis of Mössbauer spectra. *Hyperfine Interact.* **83**, 29–49.

Associate editor: W. Uwe Reimold